

# Soft and Ultra-Soft X-ray Detector Array Systems for Measurement of Edge MHD Modes in the Large Helical Device

F. WATANABE, K. TOI<sup>1)</sup>, S. OHDACHI<sup>1)</sup>, C. SUZUKI<sup>1)</sup>, S. SAKAKIBARA<sup>1)</sup>,  
K.Y. WATANABE<sup>1)</sup>, S. MORITA<sup>1)</sup>, K. NARIHARA<sup>1)</sup>, K. TANAKA<sup>1)</sup>  
and LHD experimental group<sup>1)</sup>

Department of Energy Engineering and Science, Nagoya University, Nagoya 464-8603, Japan

<sup>1)</sup>National Institute for Fusion Science, Toki 509-5292, Japan

(Received 7 December 2006 / Accepted 13 March 2007)

In the Large Helical Device (LHD), several 20-channel Soft X-ray (SX) detector arrays are used to observe the radial structures of SX fluctuations related to MHD instabilities. Recently, 20-channel absolute extreme ultraviolet (AXUV) detector arrays have also been installed inside the vacuum vessel in the vertically and horizontally elongated sections of LHD to monitor MHD fluctuations of AXUV emissions emitted from edge plasma region. These AXUV detector arrays have often detected edge MHD fluctuations localized in low temperature and density edge region so that the SX detector arrays cannot be detected. In LHD, these SX and AXUV detector array systems are successfully employed in order to investigate radial structure and temporal behaviors of edge MHD modes.

© 2007 The Japan Society of Plasma Science and Nuclear Fusion Research

Keywords: soft x-ray detector array, absolute extreme ultraviolet detector array, edge MHD mode, edge localized mode, LHD

DOI: 10.1585/pfr.2.S1066

## 1. Introduction

Soft X-ray (SX) detector array is widely used in various toroidal plasmas to measure MHD fluctuations [1–3]. This has the following advantages:

1. Compact system with multi channel detectors,
2. Fast time response,
3. Easy installation to the torus,
4. No strict limitation for plasma density and magnetic field strength.

In tokamak and helical device plasmas, edge MHD instabilities are often excited by the steep edge pressure gradient, typically realized in plasma with edge transport barrier (ETB). In LHD, edge MHD modes such as  $m/n = 1/1$ ,  $3/4$ ,  $2/3$  and  $1/2$  modes ( $m$  and  $n$ ; poloidal and toroidal mode number, respectively) are typically observed in high beta plasma as well as ETB plasmas with L-H transition [4]. The radial structures of these MHD edge modes were measured in high beta plasma [5] and ETB plasma by using 20-channel SX detector arrays [6]. The rational surface of these edge MHD modes are located near the last closed flux surface (LCFS) or the ergodic region outside LCFS. Suppression of these edge MHD modes driven by edge pressure gradient is crucial for generating high performance plasma in LHD. Therefore, it is important to clarify the characteristics of the edge MHD modes and the effects of the plasma confinement.

Recently, 20-channel absolute extreme ultraviolet (AXUV) detector arrays without beryllium foil have been

installed in LHD to monitor MHD fluctuations in very edge region. The AXUV array has already used to measure plasma radiation power and impurity ions [7–9].

## 2. SX and AXUV Array Detector Systems

SX detector array manufactured by Hamamatsu Photonics is an integral design of detector and pre-amplifier [10]. AXUV detector array manufactured by International Radiation Detectors is a design only of detector [11]. The AXUV array was built to measure light in VUV region. Figure 1 shows the sensitivity of AXUV array to photons, electrons and hydrogen ions energies referred to ref. [11]. We have used AXUV array with pre-amplifier made by

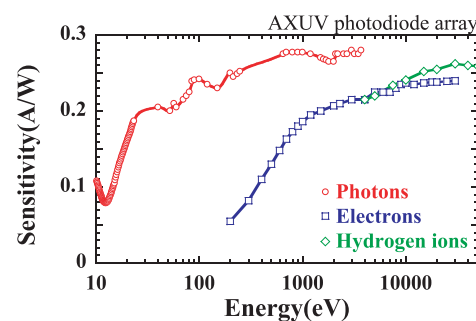


Fig. 1 The sensitivity of AXUV array to photons, electrons and hydrogen ions energies [11].

author's e-mail: fntk-w@nifs.ac.jp

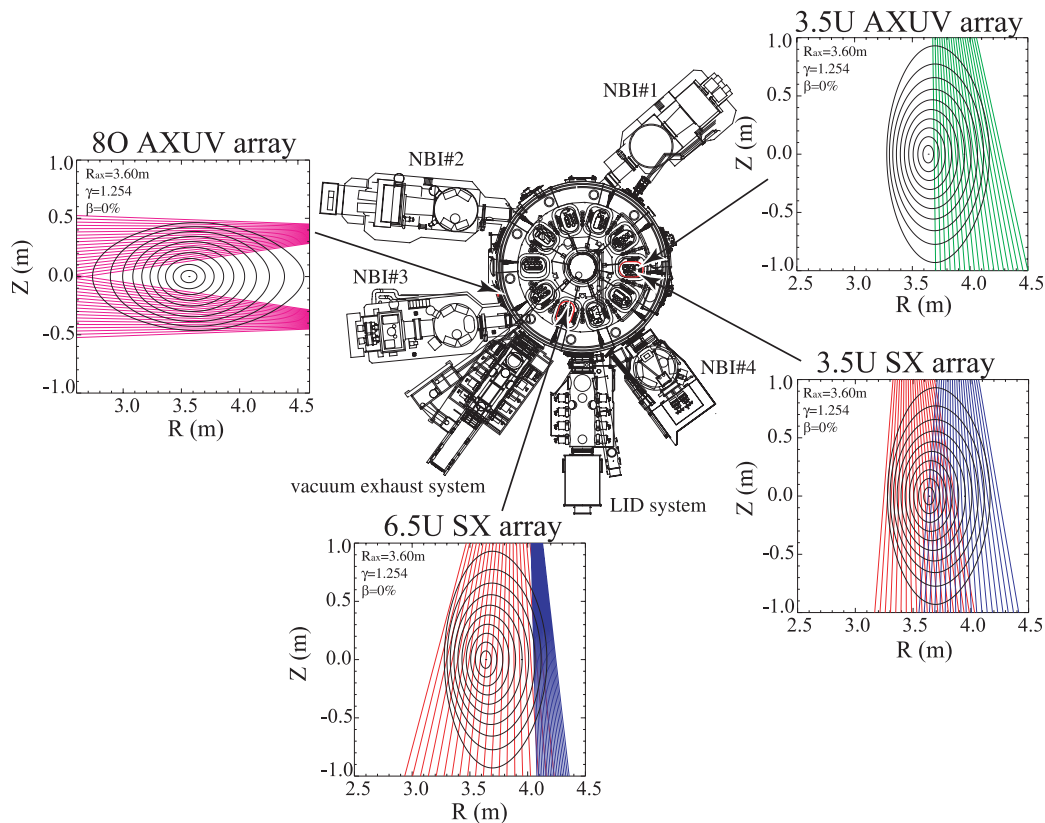


Fig. 2 SX and AXUV array systems in LHD. These systems are constituted by 4 sets of SX array and 3 sets of AXUV array. Total lines of sight are 140 channels.

Table 1 Sensitive area of SX and AXUV aetector surface

Array	Channel Number	Sensitive Area [mm <sup>2</sup> ]
SX	20ch	$1.5 \times 12 = 18$
AXUV	20ch	$0.75 \times 4 = 3$

Clear Pulse Inc. For direct conversion of photoelectric current into voltage, SX and AXUV pre-amplifier are used with a fixed conversion ratio of  $10^4$  V/A and  $10^5$  V/A, respectively. Also, AXUV photodiodes do not need external negative bias for operation. Therefore, AXUV detector is strong for electrical noise introduced through a circuit of a bias power supply, e.g. surge voltage caused by breakdown of high voltage power supplies for neutral beam injector (NBI) systems. Table 1 shows the sensitive area of the SX and AXUV detector surfaces installed on LHD, and the channel number having in the array. On the SX detector array, a beryllium foil with  $8\ \mu\text{m}$  or  $15\ \mu\text{m}$  thickness is attached in the front of the system to shut a radiation in the low photon energy region ( $E_c \lesssim 1.09\ \text{keV}$  or  $1.34\ \text{keV}$ ). On the contrary, a front of AXUV detector array is installed no beryllium foil. The AXUV array has almost constant and high sensitivity in the energy range ( $> 25\ \text{eV}$ ) from VUV to SX. Then, the sensitivity is rapidly decreased in longer wavelength range from VUV range ( $< 25\ \text{eV}$ ). Therefore,

the AXUV detector array could be detected from VUV range ( $25\ \text{eV}$ - $124.2\ \text{eV}$ ) to SX range ( $200\ \text{eV}$ - $10\ \text{keV}$ ). Note that, the sensitivity is surely existed in visible light. However, in LHD, the AXUV detector array without beryllium foil does not detect any visible light such as the  $H_\alpha$  light. That is, the time evolution of AXUV signal does not exhibit any peak observed in  $H_\alpha$  signal at the plasma initiation.

Figure 2 shows the arrangements of the SX and AXUV detector array systems in LHD. These systems are constituted by 4 sets of SX detector array and 3 sets of AXUV detector array, where each array consists of 20-channel photodiodes. They are installed inside the vacuum vessel in vertically and horizontally elongated sections of LHD. Total lines of sight are 140 channels. The viewing sight of each detector array is adjusted through a pinhole slit. The arrangement of these detectors was done, being focused on the measurement of edge plasma region. A quadrangular pinhole is placed in front of these SX and AXUV detector arrays in order to ensure good radial separation and avoid overlapping the viewing sight zone for each channel.

### 3. Experimental Results

Typical waveforms of L-H transition discharge in LHD are shown in Fig.3, where the absorbed heating

power of NBI is Co-injection (#2) and Counter-injection (#1+#3) at the toroidal field  $B_t = 0.75$  T, where the magnetic axis position of the vacuum field is  $R_{ax} = 3.6$  m and  $\gamma = 1.22$  ( $\gamma$ ; an index of the aspect-ratio of the last closed magnetic surface). Small amounts of argon (Ar) gas puff for ion temperature measurement increases edge SX emission light  $I_{SX}$  (Fig. 3 line (A)). In addition, neon (Ne) short gas puff clearly increases edge  $I_{SX}$  (Fig. 3 line (B)). In Fig. 3 line (C), edge AXUV emission light  $I_{AXUV}$  increases with the increase in line averaged electron density by the L-H transition. It should be noted that  $I_{AXUV}$  evolves in time similarly to that of the volume averaged beta  $\langle\beta_{dia}\rangle$ . On the other hand, as shown in Fig. 3 line (D), the  $I_{SX}$  intensity decreases from the saturation of the  $\langle\beta_{dia}\rangle$  after the L-H transition. This cause can be explained as below. As described in Sec. 2, the SX and AXUV detector arrays are installed with and without attaching a beryllium foil, respectively. Then, these path integrated SX and AXUV signals due to Bremsstrahlung and radiative recombination emissions will be proportional as Eqs. (1) and (2),

$$I_{SX} \propto \int_l n_e^2 \zeta \sqrt{T_e} \exp\left(-\frac{E_c}{T_e}\right) dl \quad (1)$$

$$I_{AXUV} \propto \int_l n_e^2 \zeta \sqrt{T_e} dl \quad (2)$$

where  $\zeta$ ,  $E_c$  and  $l$  are the enhancement factor for Bremsstrahlung from hydrogen plasma, cutoff energy by beryllium foil and path length of SX and AXUV detector array, respectively. As shown in Eqs. (1) and (2), SX and AXUV emission depends on electron temperature, electron density and impurity contents. The slight decrease in edge  $I_{SX}$  is thought to be due to the slight decrease in edge electron temperature caused by strong rise in edge electron density after the L-H transition as shown in Fig. 3, because  $T_e$  in the edge is much less than  $E_c \sim 1$  keV. In contrast to the edge SX signal, the increase in edge  $I_{AXUV}$  is thought to be due to the increase in edge electron density because of  $T_e \gg E_c$  for the AXUV detector.

Radial information of an edge MHD mode ( $m/n = 2/3$ ) observed by the SX and AXUV detector arrays on the vertically elongated sections of 6.5U and 3.5U ports is shown in Fig. 4 as a function of the major radius where the line sights of the SX and AXUV detector arrays intersect with the mid-plane of LHD. Here, the magnetic surfaces for  $\beta = 0.14\%$  and  $2.07\%$  are shown in Figs. 4(A-C). The SX detector array monitoring the whole plasma in the 6.5U port section gives for the overall structure of the edge MHD modes (Fig. 4(A)). The outer edge region of the LHD plasma in the 3.5U port section is measured by both the SX and AXUV detector arrays having a similar viewing sight as shown in Figs. 4(B, C). Figures 4 (D-F) show the SX and AXUV intensity profiles and the fluctuation profiles of the  $m/n = 2/3$  mode, where these SX and AXUV fluctuations  $\delta I$  have a high coherence with the magnetic fluctuations (Figs. 4(G-I)). How-

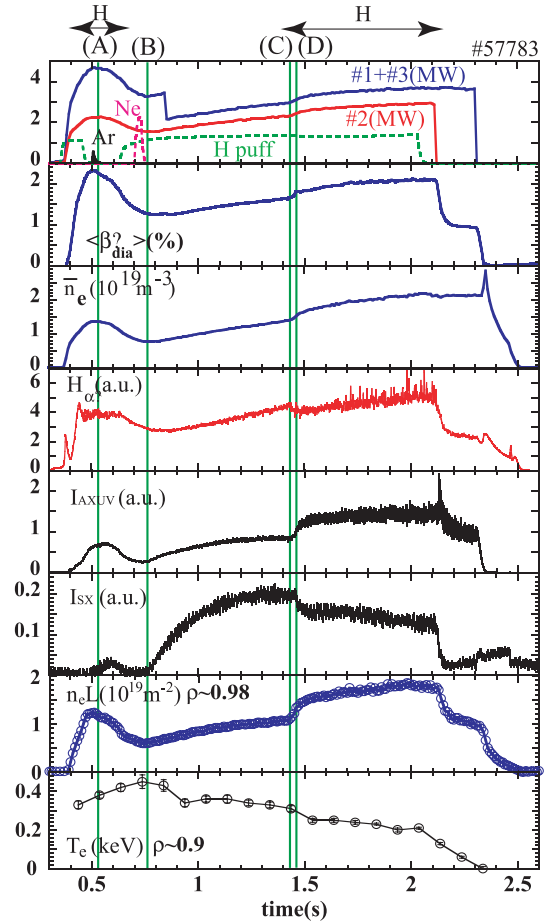


Fig. 3 Typical L-H transition discharge waveform of NBI deposition power, input gas puff, volume averaged beta value  $\langle\beta_{dia}\rangle$ , line averaged density  $\bar{n}_e$ , visible light  $H_\alpha$ , radiation loss, impurity emission, edge AXUV emission light  $I_{AXUV}$ , edge SX emission light  $I_{SX}$ , edge line integrated electron density  $n_e L$  ( $\rho \sim 0.98$ ) and edge electron temperature  $T_e$  ( $\rho \sim 0.91$ ).

ever, several channels have a low coherence because of cancellation by the path integral effect of the line of sight. This cancellation effect is often given important information of the edge MHD mode pattern. In addition, the phase difference among these channels gives an information of the mode structure, that is, the ‘even’ or ‘odd’ character of the poloidal mode number  $m$  (Fig. 4 (G-I)), where the phase difference between the SX channels at the inboard and outboard plasma edge is  $\sim 2\pi$  ( $\sim \pi$ ) for an even (odd)  $m$  number. Also, the edge AXUV emission in the low temperature and density plasma region can be detected, having significant DC and fluctuation level, which cannot detect the SX emission (Fig. 4 (D-F)).

## 4. Summary

In LHD, the AXUV detector array systems were installed for measurements of edge MHD modes in addition to the SX detector array systems. The AXUV fluctuations behave similarly to the SX fluctuation related to MHD

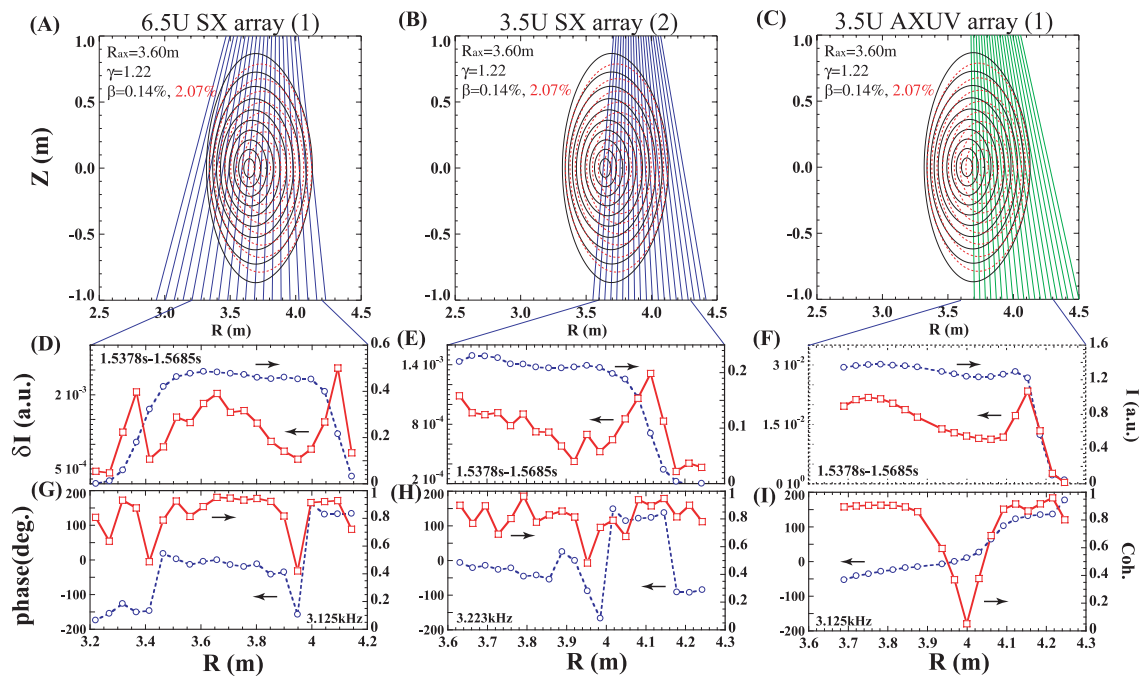


Fig. 4 (A-C) Viewing sight of SX and AXUV detector arrays on 6.5U and 3.5U port. (D-F) SX and AXUV emission profile  $I$ , fluctuation profile of edge MHD mode ( $m/n = 2/3$ )  $\delta I$ . (G-I) Phase between each SX channel and coherence with magnetic fluctuation.

instabilities. The AXUV fluctuation amplitudes are often clearer than the SX fluctuation ones, i.e. AXUV detector array is suitable for the measurement of the low electron temperature and low density edge plasmas. The emission signal from the SX with beryllium foil is sensitively dependent on electron temperature because of low edge  $T_e$ , while the signal from the AXUV detector array without the foil is mostly dependent on the products of electron density and impurities. This different sensitivity should be reminded for both SX and AXUV detector array on LHD. Nevertheless, the combination of the SX detector array and the AXUV one is concluded to be very powerful for investigation of edge MHD instabilities observed in high beta plasma and ETB plasmas in LHD.

## Acknowledgments

This work is supported in part by the LHD project budget (NIFS05ULHH508) and by the Grant-in-Aid for Scientific Research (A) from JSPS, No. 15206107.

- [1] A. Weller *et al.*, Rev. Sci. Instrum. **70**, 484(1999).
- [2] S. Ohdachi *et al.*, Rev. Sci. Instrum. **72**, 727(2001).
- [3] S. Takagi *et al.*, Phys. Plasmas **11**, 1537(2004).
- [4] K. Toi *et al.*, Phys. Plasmas **12**, 020701-1 (2005).
- [5] F. Watanabe *et al.*, J. Plasma Fusion Res. **81**, 968 (2005).
- [6] F. Watanabe *et al.*, Plasma Phys. Control. Fusion **48**, A201 (2006).
- [7] R.L. Boivin *et al.*, Rev. Sci. Instrum. **70**, 260 (1999).
- [8] Y. Liu *et al.*, Rev. Sci. Instrum. **74**, 2312 (2003).
- [9] C. Suzuki *et al.*, Rev. Sci. Instrum. **75**, 4142 (2004).
- [10] <http://jp.hamamatsu.com/index.html>
- [11] <http://www.ird-inc.com/>